JLB

Brief Conclusive Report

G protein-coupled receptor kinase-3-deficient mice exhibit WHIM syndrome features and attenuated inflammatory responses

Teresa K. Tarrant,[,1] Matthew J. Billard,* Roman G. Timoshchenko,* Marcus W. McGinnis,* D. Stephen Serafin,* Oded Foreman,[†] Denise A. Esserman,[‡,§] Nelson J. Chao,[‖] William E. Lento,[‖] David M. Lee,[¶,**] Dhavalkumar Patel,*[,***] and David P. Siderovski[††]*

*Thurston Arthritis Research Center and the Department of Medicine, Division of Rheumatology, Allergy, and Immunology, and [‡]Department of Medicine, Division of General Medicine and Clinical Epidemiology, University of North Carolina School of Medicine, Chapel Hill, North Carolina, USA; [†]The Jackson Laboratory, Sacramento, California, USA; [§]Department of Biostatistics, University of North Carolina Gillings School of Global Public Health, Chapel Hill, North Carolina, USA; [‖]Adult Stem Cell Transplant Program, Division of Cellular Therapy, Department of Medicine, Duke University Medical Center, Durham, North Carolina, USA; [¶]Brigham and Women's Hospital, Division of Rheumatology, Allergy, and Immunology, Boston, Massachusetts, USA; **Novartis Institutes for BioMedical Research, Basel, Switzerland; and [††]Department of Physiology and Pharmacology, West Virginia University School of Medicine, Morgantown, West Virginia, USA

RECEIVED FEBRUARY 22, 2013; REVISED JULY 22, 2013; ACCEPTED JULY 24, 2013. DOI: 10.1189/jlb.0213097

ABSTRACT

Chemokine receptor interactions coordinate leukocyte migration in inflammation. Chemokine receptors are GPCRs that when activated, are phosphorylated by GRKs to turn off G protein-mediated signaling yet recruit additional signaling machinery. Recently, GRK3 was identified as a negative regulator of CXCL12/CXCR4 signaling that is defective in human WHIM syndrome. Here, we report that GRK3−/− mice exhibit numerous features of human WHIM, such as impaired CXCL12-mediated desensitization, enhanced CXCR4 signaling to ERK activation, altered granulocyte migration, and a mild myelokathexis. Moreover, GRK3−/− protects mice from two acute models of inflammatory arthritis (K/BxN serum transfer and CAIA). In these granulocyte-dependent disease models, protection of GRK3−/− mice is mediated by retention of cells in the marrow, fewer circulating granulocytes in the peripheral blood, and reduced granulocytes in the joints during active inflammation. In contrast to WHIM, GRK3−/− mice have minimal hypogammaglobulinemia and a peripheral leukocytosis with increased lymphocytes and absent neutropenia. Thus, we conclude that the loss of GRK3-mediated regulation of CXCL12/CXCR4 signaling contributes to some, but not all, of the complete WHIM phenotype and that GRK3 inhibition may be beneficial in the treatment of inflammatory arthritis. *J. Leukoc. Biol.* 94: 1243–1251; 2013.

Introduction

Chemokine receptors are GPCRs that are critically involved in leukocyte migration [1], and their mutation can lead to altered signaling and migratory behavior, leading to immune system impairment. For example, in the autosomal-dominant human immunodeficiency syndrome WHIM, leukocytes exhibit enhanced chemotaxis toward the ligand of CXCR4 (stromal cell-derived factor 1 or CXCL12) and impaired CXCR4 desensitization and internalization [2]. The most-affected WHIM kindreds possess functional mutations in the carboxy terminus of the CXCR4 chemokine receptor [3]. However, two unrelated WHIM humans ("WHIM-WT" patients) have been described with normal *CXCR4* gene status [4]. These WHIM-WT subjects possess unique, functional defects in GRK3 that when corrected, lead to a restoration of normal CXCR4 internalization kinetics [4].

GRKs phosphorylate the carboxy terminus of chemokine receptors and other GPCRs in an agonist-dependent fashion [5, 6]. Agonist-activated GPCR signaling is turned off by intracellular GRKs through a process known as homologous desensitization, leading to uncoupling from heterotrimeric G pro-

Abbreviations: −/−=deficient, APC=allophycocyanin, BM=bone marrow, CAIA=collagen antibody-induced arthritis, CMP=common myeloid progenitor, df=degrees of freedom, GMP=granulocyte myeloid progenitor, Gr-1=granulocyte receptor 1, GRK=GPCR kinase, HSC=hematopoietic stem cell, IDUA=iduronidase, α-L-, K/BxN=mice expressing the TCR transgene KRN and the MHC class II molecule A(g7), LR=likelihood ratio, LSK=lineage− Sca-1+ c-Kit+, LT-LSK=long-term lineage− Sca-1+ c-Kit+, LTB4=leukotriene B4, MOMA2=anti-monocyte and macrophage antibody, PB=Pacific Blue, qRT-PCR=quantitative real-time PCR, WHIM=warts, hypogammaglobulinemia, infections, myelokathexis, WHIM-WT=warts, hypogammaglobulinemia, infections, myelokathexis patients with a normal CXCR4 ORF

1. Correspondence: University of North Carolina at Chapel Hill, CB #7280, 3300 Manning Dr., Chapel Hill, NC 27599, USA. E-mail: tarra002@med.unc.edu

0741-5400/13/0094-1243 © Society for Leukocyte Biology

teins and receptor internalization that is facilitated further through the binding of β-arrestin [5, 6]. As it pertains to leukocyte trafficking, this negative-feedback loop is important in the regulation of chemokine receptor signaling and surface expression and thus, in determining how leukocytes move in homeostatic and proinflammatory conditions.

Among the seven GRK family members, there is a high degree of sequence homology [6], as well as overlapping tissue prevalence [7]. Whereas it is often assumed that structural and expression pattern similarities translate into functional overlap, clear, functional differences have been identified among highly related GRKs. With respect to CXCR4 signaling in the human embryonic kidney 293 cell line, GRK2 serves as a negative regulator of agonist-dependent ERK1/2 activation, whereas GRK3 and -6 are observed to positively regulate ERK1/2 output from CXCL12 activation; importantly, different residues are phosphorylated within activated CXCR4 by each of these kinases [8, 9]. Other biochemical studies have found that compared with WT CXCR4, WHIM-mutant CXCR4 receptors that lack the carboxy-terminal 19 residues internalize and activate ERK1/2 more slowly; GRK6 but not GRK3 fails to associate with this particular mutant receptor [10]. Thus, compelling data exist to support GRK2, -3, and -6 having differential effects on the regulation of CXCR4 and its output to MAPK/ERK signaling [4, 8, 10].

Given that GRK3 defects have been associated with CXCR4 dysregulation and clinical WHIM in humans [4], our hypothesis was that GRK3−/− mice would exhibit similar immunologic phenotypes. In GRK3−/− mice, CXCR4 receptor internalization and ERK signaling were prolonged in immune cells consistent with WHIM [2]. Additionally, GRK3−/− mice had increased granulocytes in the BM and reduced numbers of neutrophils in the blood but only during pronounced inflammation in granulocyte-dependent disease models of inflammatory arthritis. GRK3−/− mice had minimal hypogammaglobulinemia, which has been reported as variable in WHIM patients [11, 12]. However, in clear contrast to patients with WHIM [11, 12], neutropenia was not present at baseline in GRK3−/− mice, and a notable lymphocytosis in the peripheral blood was found to persist at baseline and during active inflammation in GRK3−/− mice. These data suggest that GRK3 may regulate signaling pathways that lead to specific immune cell functions that differ between granulocytes and lymphocytes and that GRK3−/− alone in mice does not fully recapitulate the complete WHIM phenotype. Our data suggest that this selective immunoregulation may be advantageous in autoimmune-mediated inflammation, such as inflammatory arthritis.

MATERIALS AND METHODS

Animals

The GRK3−/− mouse strain [13–15] was kindly provided by Dr. Robert J. Lefkowitz (Duke University, Durham, NC, USA). GRK3−/− (>12 generations back-crossed) and WT age-matched male C57Bl/6 mice were used for all experiments under standard Institutional Animal Care and Use Committee-approved protocols in the Association for Assessment and Accreditation of Laboratory Animal Care-accredited vivarium of the University of North Carolina.

Inflammatory arthritis models

K/BxN was induced by injecting 5 μl/g mouse weight i.p., with sera pooled from K/BxN transgenic mice on Days 0 and 2, per our previously published protocol [16]. CAIA was induced by injecting 5 mg/mouse i.p. of arthrogenic mAb (Chondrex, Redmond, WA, USA) 5-clone cocktail on Day 0, followed by 50 mg i.p. LPS on Day 3, according to manufacturer instructions. Mice were measured by a blinded observer for (1) a clinical disease score index and (2) measurement of paw swelling from baseline. The clinical disease score index was performed with the following scoring system: 0 = normal paw; 1 = mild but definite swelling of the ankle or digits; 2 = moderate redness and swelling of an ankle ± any number of digits; 3 = maximal redness and swelling of the entire paw and digits, with or without ankylosis. The maximum score/paw was 3, with a total score obtainable of 12/mouse. Paw swelling was measured by calipers and assessed daily as the millimeter swelling over baseline; both scoring methods have been published previously and validated by our group in inflammatory arthritis models [16].

Chemotaxis

Transendothelial migration assays were performed with EA.hy926 endothelial cell-coated, 5 μm pore-sized Transwells. The migration of BM-derived granulocytes, in response to media or chemokine ligands (PeproTech, Rocky Hill, NJ), was determined by anti-Ly6G staining and flow cytometry analysis of migrated cells into the lower chamber, as per our previously published protocol [16].

BM analysis

For histopathology, two femurs/animal were isolated and fixed for 24 h in Tellyesnickzky/Fekete fixative, decalcified using EDTA, and embedded in paraffin. Serial, 5- to 7-mm sections were stained with H&E and analyzed by a blinded veterinary pathologist for morphologic analysis using an Olympus Bx41 microscope. Images were captured with an Olympus DP72 camera using CellSens imaging software. The objective used for the images in marrow studies (see Fig. 2) was 40×. For each sample, 200 cells were counted and classified by type and stage. The myeloid:erythroid ratio was calculated by dividing the number of myeloid precursor cells by the number of erythroid precursor cells, according to reports published previously [17]. For hematopoietic cell-count analysis of the BM, both femurs and tibias/mouse were flushed, and red cells were lysed. With the use of trypan exclusion, total viable hematopoietic cells were counted manually by a hemocytometer for a total cell count. Hematopoietic, mature subsets from the BM were defined by forward- and side-scatter and the following cell-surface markers: erythroid TER-119-PerCP, myeloid Gr-1-APC-Cy7 and CD11b-BV421, lymphoid CD3-FITC and B220-PE. Antibodies were purchased from BioLegend (San Diego, CA, USA), except CD3-FITC, from BD PharMingen (San Diego, CA, USA). Cell populations were enumerated by multiplying the percent positive of forward- and side-scatter-gated cells by total BM cell counts. Granulocyte subset-gating strategy was based on Ueda et al. [18]. The lineage-negative hematopoietic cell subsets were phenotyped by excluding all lineage-positive cells (TER-119-, Gr-1-, CD11b-, CD3-, CD4-, CD8-, and B220-PeCy5), examining c-kit (eFluor780 or APC) and Sca-1 (PeCy7) populations, and then subsetting further for multipotent progenitor stem cells with CD34 (eFluor450) and CD16/32 (PE or APC) or signaling lymphocyte activation molecule stem cells with CD48 (FITC) and CD150 (APC). All antibodies were purchased by eBioscience (San Diego, CA, USA), except for CD150, which was purchased from BioLegend.

Peripheral blood analysis

Whole blood (40 μl) was stained and analyzed by FACS using BD TruCOUNT tubes for absolute cell counts, adapted from protocols published previously [19] and manufacturer's instructions. Cell populations analyzed

included total cell count (CD45-PerCP or -APC-Cy7), B cells (B220-PeCy7 or -PB), T cells (CD3-PE or -PB), monocytes (MOMA2-FITC), and neutrophils (LyG-PECy5, -FITC, or -PE). Antibodies were purchased from BD Biosciences (San Jose, CA, USA), except for MOMA2, which was provided by Beckman Coulter (Brea, CA, USA); CD3-PE or Ly6G-PeCy5, purchased from Abcam (Cambridge, MA, USA); and CD3-PB, purchased from BioLegend.

qRT-PCR

Total RNA was prepared using a Qiagen RNeasy genomic-free kit and cDNA synthesized with Superscript II RT (Invitrogen, Carlsbad, CA, USA), followed by qRT-PCR. Both 18S and IDUA served as reference genes, per our primer sequences and protocol published previously [20]. For MPO, the following primers were used: forward 5′-ATC ACG GCC TCC CAG GAT ACA ATG-3′ and reverse 5′-ACC GCC CAT CCA GAT GTC AAT G-3′. For elastase, the following primers were used: forward 5′-CCT TCT CTG TGC AGC GGA TCT TC-3′ and reverse 5′-ACA TGG AGT TCT GTC ACC CAC-3′.

GPCR internalization assay

Ableson virus-immortalized pre-B cells [21] were derived from GRK3−/−, GRK5−/−, and WT BM. To quantitate internalization, we adapted from previously published protocols [2]. Briefly, cells lines were stimulated with 200 nM CXCL12 (Shenandoah Biotechnology, Warwick, PA, USA) or media, washed in ice-cold glycine-HCl-NaCl buffer, and then stained for surface expression of CXC4 (R&D Systems, Minneapolis, MN, USA) and analyzed by flow cytometry. Cells were kept in ice-cold reagents and at 4°C after ligand stimulation to arrest further internalization. Data are expressed as percent change in surface expression of CXCR4 compared with baseline in media.

Western immunoblotting

Standard protocols were used with dilutions of phospho-ERK1/2 (1:1,000) and total ERK1/2 (1:1,000) primary antibodies (Cell Signaling Technology, Danvers, MA, USA) on cell lysates of primary BM cells after incubation with 1 μg/ml CXCL12 (Shenandoah Biotechnology).

Serum Igs

Total levels of Igs, IgM, IgA, IgE, IgG, and subclasses IgG1, IgG2a, IgG2b, IgG2c, and IgG3, were quantitated by ELISA from naive mouse sera, according to the manufacturer's instructions (Immunology Consultants Laboratory, Newberg, OR, USA).

Statistical analyses

For clinical disease and paw-swelling curves, linear mixed models were used as described previously [16, 20]. The overall group effect was assessed using a LR test (α=0.05) with SAS v9.2. For qRT-PCR, flow cytometry, ELISA, histopathology, and chemotaxis data, a two-tailed Student's *t*-test was used with Prism v4.

RESULTS AND DISCUSSION

GRK3−/− impairs ligand-dependent CXCR4 internalization and enhances chemotaxis and ERK1/2 activation

Impaired CXCR4 internalization in the presence of the chemokine CXCL12 is observed in cells isolated from WHIM syndrome patients or mice harboring the WHIM-associated *CXCR4* mutation (i.e., *Cxcr4*$^{+/1013}$) [2, 22]. CXCL12-activated CXCR4 signaling is turned off by GRKs via homologous desensitization; the final step is receptor internalization [5, 6]. To test the specific role of GRK3 in internalization of activated CXCR4 by primary immune cells, we created BM-derived pre-B cell lines from GRK3−/− and WT mice using Abelson virus immortalization [21]; GRK5−/− pre-B cell lines were also

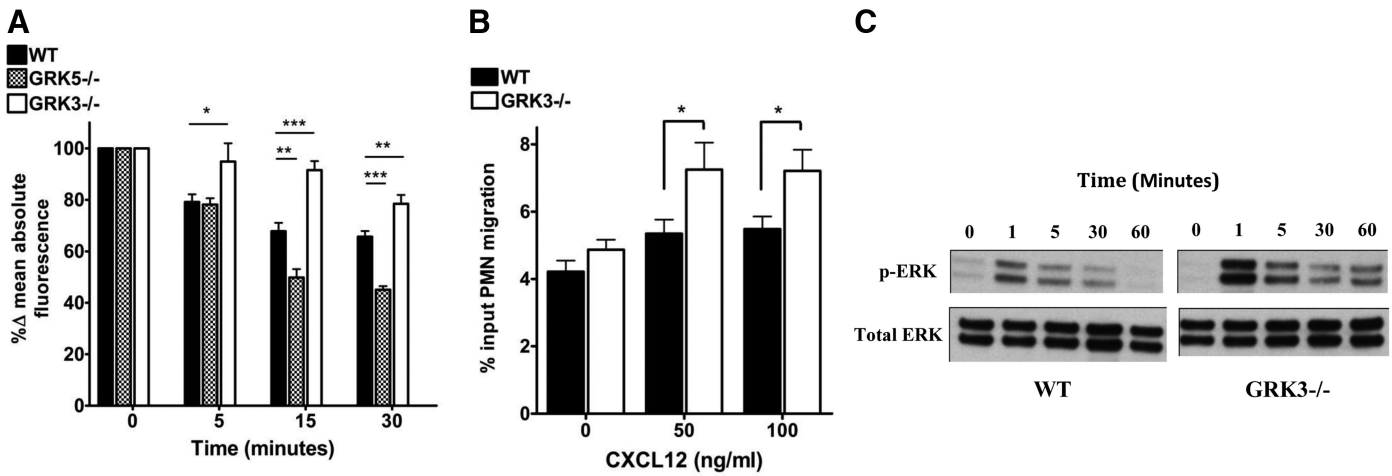

Figure 1. GRK3−/− BM-derived leukocytes have impaired CXCR4 internalization, enhanced chemotaxis, and increased ERK1/2 activation when exposed ex vivo to CXCL12. (A) Abelson virus-immortalized pre-B cells were derived from GRK3−/−, GRK5−/−, and WT BM. GRK3−/− cells (n=7) had impaired internalization of CXCR4 after exposure to 50 nM CXCL12 when compared with GRK5−/− (n=6) and WT (n=12) cells. CXCR4 receptor internalization in stimulated leukocytes was calculated as follows: receptor geometric mean fluorescence intensity of CXCL12-treated cells/receptor geometric mean fluorescence intensity of unstimulated cells − background fluorescence (*P<0.05; **P<0.01; ***P<0.001). Δ, Change. (B) Ly6G+ granulocytes isolated from BM of GRK3−/− (n=13) and WT mice (n=13) have enhanced chemotaxis to CXCL12 (50 and 100 ng/ml) in transendothelial migration assays. PMN, Polymorphonuclear neutrophil. (C) Isolated BM from GRK3−/− mice has prolonged and increased ERK1/2 activation when stimulated over 60 min with 1 μg/ml CXCL12 (represenatative of one of three experiments). The gel was not cut or enhanced. p-, Phosphorylated.

generated as an additional control, as this kinase is not thought to regulate the CXCR4 receptor [8, 9]. The cells were stimulated ex vivo with CXCL12, and the expression of surface CXCR4 over time was analyzed by flow cytometry. GRK3−/− pre-B cells exhibited sustained levels of surface CXCR4 expression after ligand stimulation, ranging from a 13–52% increase when compared with WT and GRK5−/− cells for over 30 min of observation (**Fig. 1A**).

To test for functional effects of GRK3−/− on chemotaxis, primary BM-derived cells were isolated, and Ly6G+ granulocytes were examined for their migratory behavior toward CXCL12, as granulocytes are known to migrate abnormally in WHIM [2, 4]. GRK3−/− Ly6G+ granulocytes exhibited enhanced chemotaxis to CXCL12, similar to what has been shown in WHIM and WHIM-WT patients [2, 4] when compared with WT cells ($P<0.05$; Fig. 1B). GRK3−/− B and T lymphocytes showed enhanced migration, albeit less than that of granulocytes (data not shown).

Chemokine GPCRs, when stimulated, activate the MAPK pathway, and CXCR4 receptor stimulation is known to activate ERK1/2 specifically [8, 10]. To determine whether CXCL12/CXCR4 intracellular signaling was enhanced in GRK3−/− BM as it is in WHIM [2], whole BM leukocytes were isolated, stimulated ex vivo with CXCL12, and examined for ERK1/2 activation status. GRK3−/− leukocytes showed enhanced and prolonged ERK1/2 activation compared with WT leukocytes (Fig. 1C). Thus, we have found that similar to WHIM and WHIM-WT patients, GRK3−/− in mice reveals a pivotal role for this kinase in CXCL12-promoted desensitization, internalization of CXCR4, chemotaxis, and ERK1/2 activation in immune cells.

GRK3−/− has increased granulocytes and precursors in the marrow

Myelokathexis describes the hypercellular marrow observed in WHIM, which is believed to occur by stromal-produced CXCL12 acting on CXCR4-expressing hematopoietic cells that have enhanced signaling responses and thus, do not exit the marrow into the blood [12]. Given that the CXCL12/CXCR4 signaling in the GRK3−/− mouse mirrors that of WHIM and WHIM-WT humans (Fig. 1), we chose to examine the cellular composition of BM to determine whether GRK3−/− also leads to myelokathexis. By visual inspection (**Fig. 2A** and **B**), viable cell counts of total hematopoietic cells isolated from the femurs and tibias of mice (Fig. 2C), and myeloid/erythroid ratio comparisons by histopathology of the femurs (Fig. 2D), there were more hematopoietic cells in GRK3−/− marrow compared with controls, despite similar amounts of *CXCL12* produced (Fig. 2E).

Differentiated lineage markers of BM cells, enumerating lymphoid (B220, CD3), erythroid (Terr-119), and myeloid/granulocyte subsets (Gr-1, CD11b), were increased slightly in GRK3−/− mice (**Fig. 3A**), but notably, the mature granulocyte subpopulation staining strongly for Gr-1^{hi}/CD11b^{hi} (Fig. 3B–D) was increased statistically in the BM isolates of GRK3−/− mice ($P<0.001$). GRK3 heterozygous animals were analyzed similarly and found to have an intermediate phenotype that was not statistically significant from WT controls (data not shown).

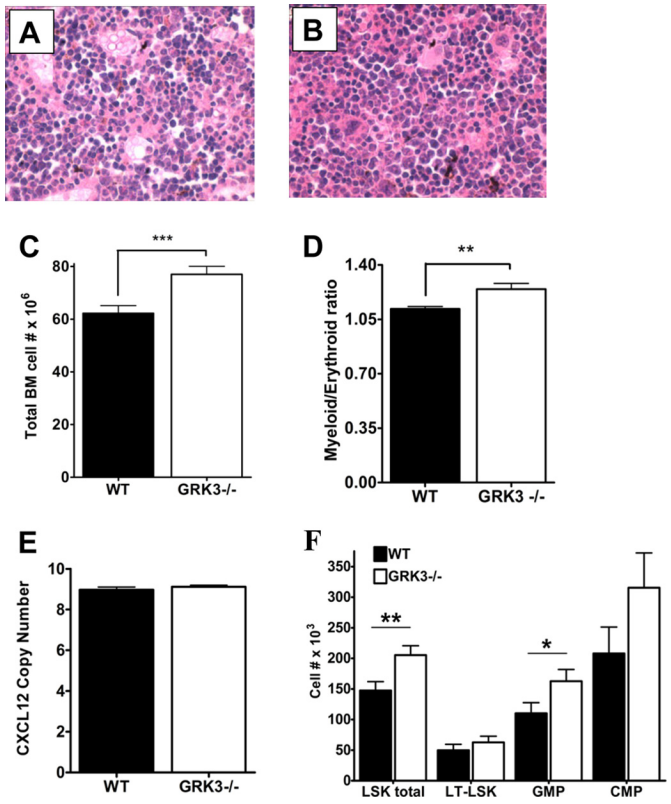

Figure 2. GRK3−/− mice have a hypercellular BM. Representative histopathology from femurs of WT (A) and GRK3−/− (B) mice show hypercellularity in GRK3−/− animals (40× original resolution). Total viable hematopoietic cells isolated from crushed femurs and tibias and assessed by trypan blue exclusion were increased in GRK3−/− mice ($n=13$) compared with WT mice ($n=14$; ***$P<0.001$, C). BM cellular morphology was scored by a blinded histopathologist, and the myeloid: erythroid ratio was found to be increased in GRK3−/− mice ($n=20$ separate femurs) compared with WT mice ($n=20$ separate femurs; **$P<0.01$, D), despite similar copy number of BM-derived CXCL12, as assessed by qRT-PCR (WT, $n=4$; GRK3−/−, $n=5$; E). (F) All subsets of Lin− HSCs from femur and tibia BM isolates of GRK3−/− mice ($n=12$) were increased, and GRK3−/− LSK (**$P<0.01$) and GMP cell numbers (*$P<0.05$) were increased statistically compared with WT ($n=13$) controls (LSK: c-kit+ Sca-1+; LT-LSK: c-kit+ Sca-1+ CD48− CD150+; GMP: c-kit+ Sca-1− CD16/32+ CD34+; CMP: c-kit+ Sca-1− CD16/32− CD34+).

Interestingly, Lin−, multipotent HSCs, defined as the LSK population, were increased statistically ($P<0.01$) in GRK3−/− mice (Fig. 2F). Similarly, the GMP (c-kit+ Sca-1− CD16/32+ CD34+) population was also increased statistically ($P<0.05$; Fig. 2F). Other HSC populations, such as the LT-LSK population (c-kit+ Sca-1+ CD48− CD150+) and the CMP population (c-kit+ Sca-1− CD16/32− CD34+), were increased but not statistically different between GRK3−/− mice and controls (Fig. 2F).

Our flow cytometry data suggest that GRK3−/− contributes to the observed, increased total numbers of HSC in the BM (i.e., myelokathexis), with a bias toward granulocytes and their

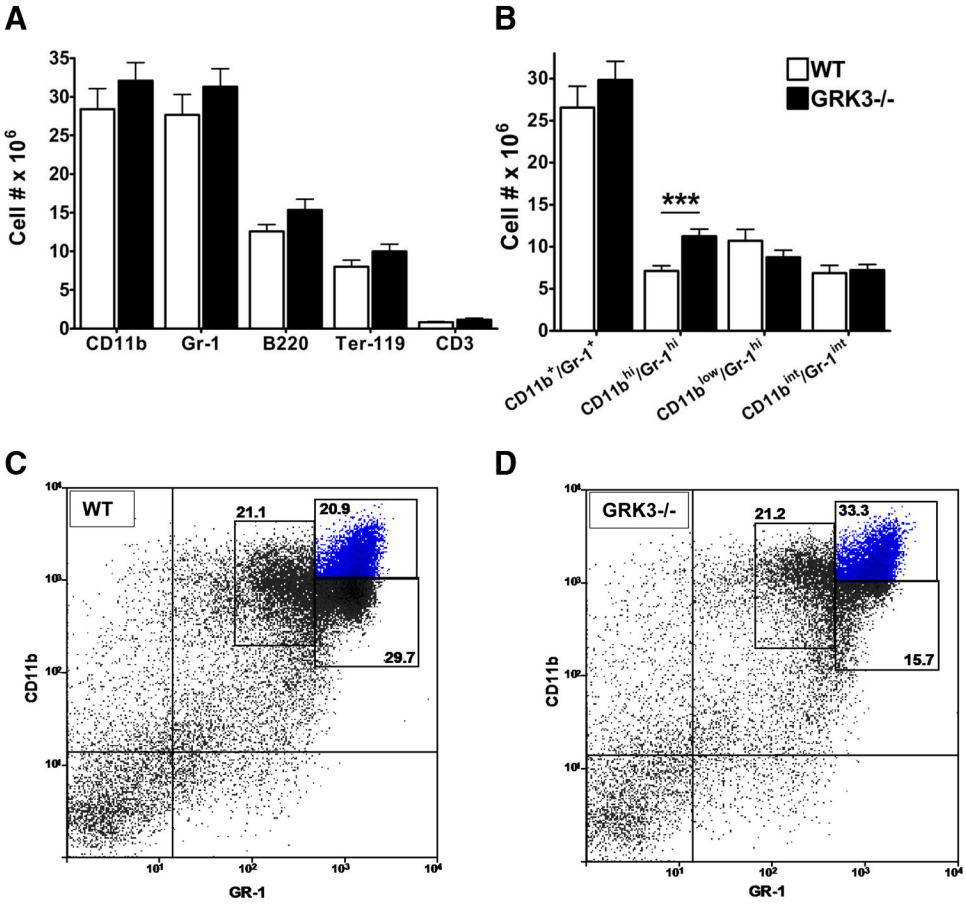

Figure 3. GRK3−/− mice have increased numbers of Gr-1^{hi}/CD11b^{hi} granulocyte subset in the BM. (A) Numbers of myeloid/granulocyte (CD11b, Gr-1), lymphoid (B220, CD3), and erythroid (Ter-119) subpopulations were determined by immunofluorescent staining and flow cytometric analysis from the BM of age- and gender-matched GRK3−/− and WT C57/BL6 mice. (B) The granulocyte subpopulation CD11b^{hi}/Gr-1^{hi} was increased significantly in GRK3−/− mice (n=9/group; data represented as mean±SEM; ***P=0.001). Representative dot plots of granulocyte subset analysis for (C) WT and (D) GRK3−/− BM.

precursors. Given the importance of CXCL12 and CXCR4 signaling in the BM niche [23] and in hematopoietic cell transplantation [24], these data also suggest a potential role for GRK3 in stromal/HSC interactions that could be manipulated therapeutically in transplantation and/or stem cell mobilization. This could be a valuable area for future study.

The overall increase in BM cellularity in GRK3−/− mice, although statistically significant, is less than what is typically seen in WHIM patients with CXCR4 mutations [11] but has clear effects that are more pronounced on granulocyte precursors and the Gr-1^{hi}/CD11b^{hi} mature subset (Figs. 2 and 3). One potential explanation is that although GRK3 regulates CXCR4 signaling through the MAPK pathway and has functional outcomes in granulocytes, some overlap likely exists with GRK2- and/or GRK6-mediated phosphorylation of activated CXCR4 and resultant recruitment of β-arrestin [8, 25]. Thus, in some granulocyte subpopulations and perhaps even more so in other mature hematopoietic subsets (i.e., lymphocyte and/or erythroid lineages), GRK2 and/or -6 may be able to compensate for the loss of GRK3 function, leading to appropriate cellular exodus from the BM.

GRK3−/− mice exhibit partial hypogammaglobulinemia

As the syndrome's name implies, hypogammaglobulinemia can be a feature of WHIM; however, variable titers of antibody isotypes have been described [12], and the exact mechanism is not well understood. We examined total IgG, IgM, IgA, and IgE, as well as IgG subclasses in GRK3−/− mice, which were largely preserved, with statistical decreases seen only in IgA, IgE, and IgG1 levels (**Table 1**). One potential explanation is

TABLE 1. GRK3−/− Mice Have Selective Hypogammaglobulinemia Compared with WT Controls

	IgG μg/mL	IgG1[a] μg/mL	IgG2a ng/mL	IgG2b μg/mL	IgG2c μg/mL	IgG3 μg/mL	IgM μg/mL	IgA[a] μg/mL	IgE[b] ng/mL
WT	927 ± 163.4	226 ± 27.2	1231 ± 29.1	2329 ± 259.0	142 ± 33.3	274 ± 28.2	1895 ± 100.9	154 ± 46.7	55.5 ± 6.9
GRK3−/−	1048 ± 65.4	158 ± 16.0	1215 ± 21.9	3310 ± 357.8	152 ± 21.2	298 ± 18.9	1842 ± 209.2	60.8 ± 7.6	37.3 ± 3.2

GRK3−/− mice (>n=15) and WT mice (n=10) were bled by tail nick at 8 weeks of age. Total IgM, IgA, IgE, IgG, and IgG subclasses IgG1, IgG2a, IgG2b, IgG2c, and IgG3 were measured from serum. IgG1, IgA, and IgE ([a]P<0.05; [b]P<0.01) were reduced significantly in GRK3−/− mice.

that GRK3 may not substantially alter B cell functions that control overall γ-globulin production or class-switching, particularly as a complete absence was not observed for any of the Ig classes or subclasses. However, the possibility exists that hypogammaglobulinemia may be more pronounced in an immunization model, in which a de novo antigen is presented, and antibodies are generated in response. Future studies investigating the quantitative and qualitative capacity of GRK3−/− B cells in de novo antibody responses will need to be performed to elucidate further this aspect of the GRK3−/− immune phenotype. Of note, it is interesting that one WHIM-WT patient, identified as P3, with decreased GRK3 mRNA and protein had "low normal" immune γ-globulins [2], which is somewhat reflective of the phenotype in GRK3−/− mice that we describe here.

GRK3−/− decreases disease sequelae in two models of acute inflammatory arthritis

The induction of antibody-induced arthritis is independent of B and T lymphocytes [26] and importantly, is highly dependent on granulocytes for disease induction and severity [27]. WHIM subjects have impaired granulocyte migration [11, 12]; therefore, we chose two complementary inflammatory arthritis models (K/BxN serum transfer and CAIA) to assess in vivo granulocyte migration and disease progression in GRK3−/− mice. In both models, GRK3−/− mice had less inflammatory arthritis by two independent measures of paw swelling ($P<0.01$ CAIA; $P<0.0001$ K/BxN; **Fig. 4A** and **C**) and clinical disease score ($P<0.0001$ CAIA; $P<0.0001$ K/BxN; Fig. 4B and D). We show additionally that GRK3−/− Ly6G+ granulocytes do not migrate differently to the proinflammatory chemokines C5a, IL-8, and LTB4 (Fig. 4E), which are known to be relevant in antibody-induced arthritis disease models, and their target GPCRs are affected by other GRKs [28]. This supported our hypothesis further that GRK3−/− granulocytes migrate to joint less (**Fig. 5B–D**) in inflammation, as they are retained in the marrow (Fig. 3B–D), where CXCL12 is produced and where there is a heightened signaling response (Fig. 1). Indeed, GRK3−/− arthritic paws had both decreased quantitative mRNA expression of key neutrophil markers, MPO, and

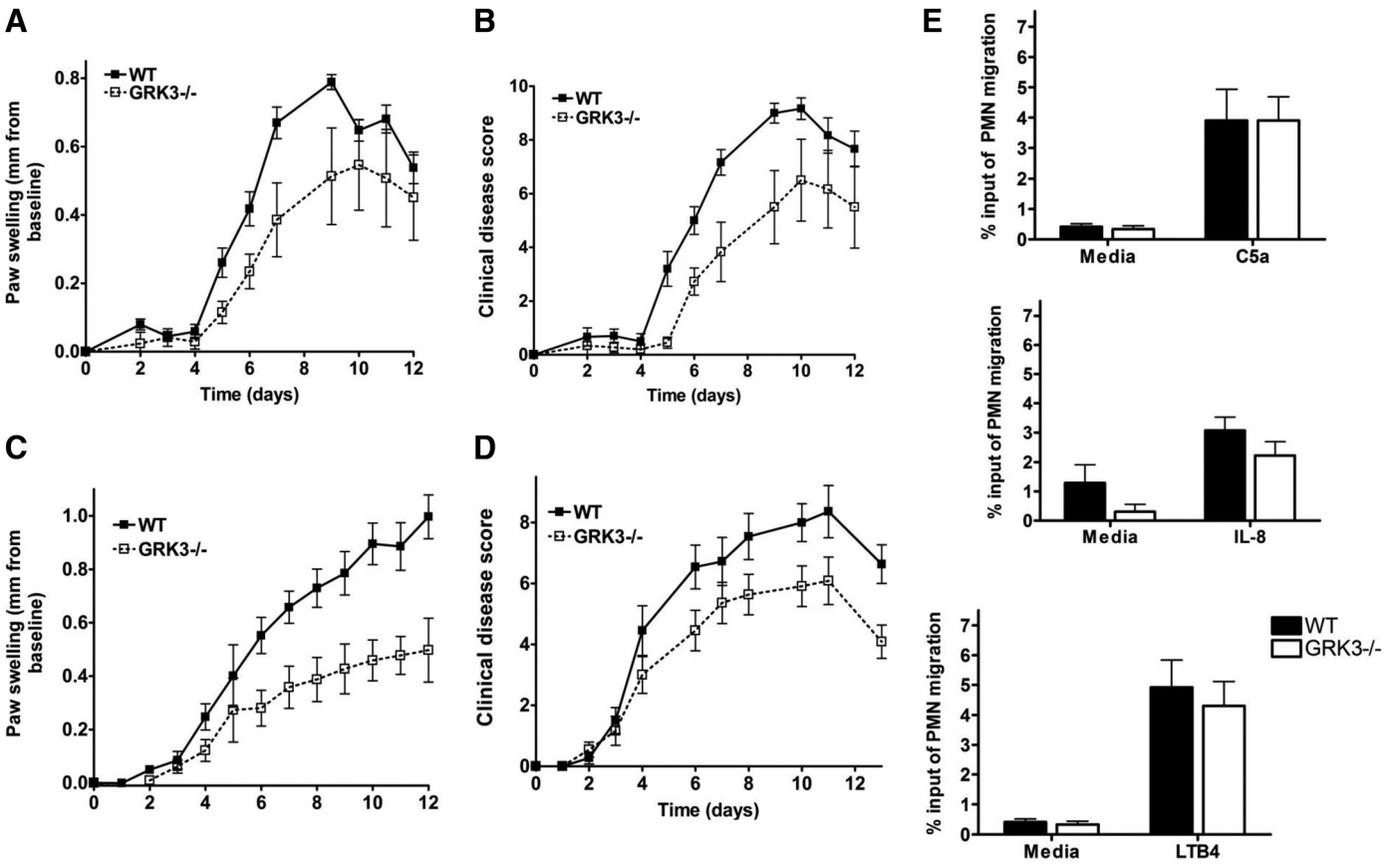

Figure 4. Acute inflammatory arthritis is decreased in GRK3−/− mice in the K/BxN serum transfer and CAIA models, despite similar trafficking to proinflammatory chemokines. Significant decreases were observed in paw swelling (A, CAIA; C, K/BxN) and clinical disease (B, CAIA; D, K/BxN) between GRK3−/− mice and WT controls. Paw-swelling data represent mean difference in millimeters from baseline thickness of the ankles ± SEM over time (CAIA: LR=13.5, df=3, $P<0.01$; K/BxN: LR=90.3, df=3, $P<0.0001$). Clinical disease data are based on a 0–3 grading for each paw (CAIA: LR=23.4, df=3, $P<0.0001$; K/BxN: LR=28.7, df=2, $P<0.0001$). Each figure represents two independent experiments with a total of 11 mice/group. (E) Transendothelial migration assays of Ly6G+ granulocytes in response to 10 nM LTB4, 100 nM C5a, and 100 μg/ml IL-8. Data are represented as percent migration of the total input ± SEM; $n = 6$ experiments for each chemokine ligand, and there was no statistical difference in migration between GRK3−/− and WT mice.

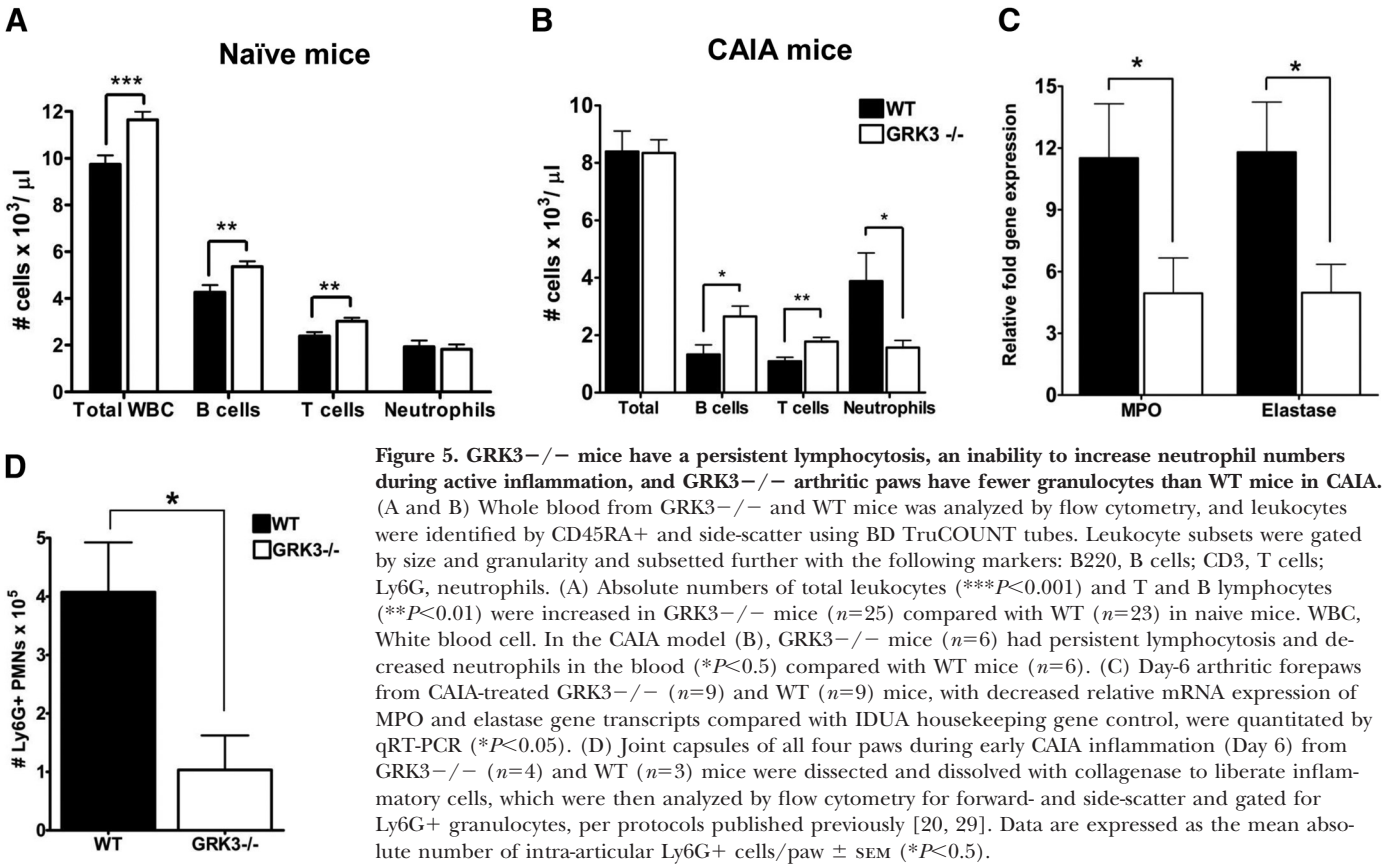

Figure 5. GRK3−/− mice have a persistent lymphocytosis, an inability to increase neutrophil numbers during active inflammation, and GRK3−/− arthritic paws have fewer granulocytes than WT mice in CAIA. (A and B) Whole blood from GRK3−/− and WT mice was analyzed by flow cytometry, and leukocytes were identified by CD45RA+ and side-scatter using BD TruCOUNT tubes. Leukocyte subsets were gated by size and granularity and subsetted further with the following markers: B220, B cells; CD3, T cells; Ly6G, neutrophils. (A) Absolute numbers of total leukocytes (***$P<0.001$) and T and B lymphocytes (**$P<0.01$) were increased in GRK3−/− mice ($n=25$) compared with WT ($n=23$) in naive mice. WBC, White blood cell. In the CAIA model (B), GRK3−/− mice ($n=6$) had persistent lymphocytosis and decreased neutrophils in the blood (*$P<0.5$) compared with WT mice ($n=6$). (C) Day-6 arthritic forepaws from CAIA-treated GRK3−/− ($n=9$) and WT ($n=9$) mice, with decreased relative mRNA expression of MPO and elastase gene transcripts compared with IDUA housekeeping gene control, were quantitated by qRT-PCR (*$P<0.05$). (D) Joint capsules of all four paws during early CAIA inflammation (Day 6) from GRK3−/− ($n=4$) and WT ($n=3$) mice were dissected and dissolved with collagenase to liberate inflammatory cells, which were then analyzed by flow cytometry for forward- and side-scatter and gated for Ly6G+ granulocytes, per protocols published previously [20, 29]. Data are expressed as the mean absolute number of intra-articular Ly6G+ cells/paw ± SEM (*$P<0.5$).

elastase (Fig. 5C), and Ly6G+ cells were decreased in number by flow cytometry (Fig. 5D). Thus, our findings that GRK3−/− have attenuated inflammatory arthritis by having heightened granulocyte responses to CXCL12 produced in the marrow and not to C5a, IL-8, and LTB4 produced at the site of inflammation may be advantageous with respect to autoimmunity. Kinase inhibition is becoming established as an effective therapeutic strategy in rheumatoid arthritis [30], and future studies of GRK3 inhibition in preclinical autoimmune models and in the regulation of other chemokine GPCRs may be warranted.

GRK3−/− mice exhibit lymphocytosis at baseline and during active inflammation

GRK3−/− mice produce normal litters, live a normal lifespan, have normal immune organogenesis, do not exhibit any obvious clinical phenotype when housed in pathogen-free conditions, and are unchallenged by inflammatory stimuli (data not shown). Despite not being challenged with obvious infectious pathogens, naive GRK3−/− mice demonstrate a leukocytosis with expansion of T and B lymphocytes in the peripheral blood at baseline (Fig. 5A). This expansion is leukocyte subtype-specific in that granulocytes are similar in number in the unchallenged, naive state between GRK3−/− mice and controls (Fig. 5A). Only during active inflammation are neutrophils decreased in the peripheral blood of GRK3−/− mice relative to WTs, whereas lymphocytes continue to be elevated (Fig. 5B). This observation suggests that GRK3-mediated regulation of GPCR signaling may have differential effects in different leukocyte subsets, a phenomena that has been observed in other GRK3−/− strains. Specifically, studies using GRK6−/− mice have demonstrated a positive regulatory role of GRK6 in T cell chemotaxis toward CXCL12, whereas an opposite effect is observed in neutrophils [31, 32]. GRK2 and -3 do not phosphorylate the same serine/threonine residues of the CXCR4 receptor as GRK6 [8], suggesting differential modulation of CXCL12/CXCR4 signaling and the potential for different cellular outcomes. CXCR4 signaling is critical to lymphopoiesis, as CXCR4−/− leads to an absence of B cell and granulocyte formation [33]. Thus, it is conceivable that GRK3 has a more pronounced effect on granulocyte trafficking in response to CXCL12/CXCR4 interactions (as also suggested by our marrow studies of Figs. 2 and 3), whereas differentiation, maturation, and migration may be differentially affected in lymphocyte lineages in the absence of GRK3 expression.

Previous studies examining GRK3−/− mice have demonstrated a physiologic role for GRK3 in the regulation of olfactory, M2/M3 muscarinic, and κ-opioid receptor function [13–15]. However, to date, no assessment of immune system impairment has been made in this mouse strain since the discovery of WHIM syndrome and identified patients with decreased GRK3 function yet wild-type *CXCR4* gene status ("WHIM-WT" patients) [2, 4]. The specific clinical phenotype of GRK3-defective WHIM-WT patients is reported to include myelokathexis and neutropenia [11], yet their precise molecular defect remains unclear, as the *GRK3* [4] ORF was also found to be of WT sequence in these patients. Interestingly,

WHIM-WT P3 had decreased GRK3 mRNA and protein, suspected to result from a post-transcriptional defect [4]. P3 had a milder form of neutropenia and low normal immune γ-globulins [2], reflective of our findings in the GRK3−/− mouse. Clinical manifestations for the P4 WHIM-WT patient included additional characteristics of severe infection with human papilloma virus [11], hypogammaglobulinemia, and lymphopenia, in addition to severe neutropenia [34], but this patient had normal *GRK3* ORF, mRNA, and protein [4]. Thus, whereas cells from patient P4 had defects that were restored in vitro by GRK3 overexpression [4], the precise molecular defect of this patient may not involve GRK3 directly per se. Therefore, our phenotypic analysis of the GRK3−/− mouse provides interesting insight into the absolute GRK3−/− and its effects on hematopoiesis that provide additional information beyond the two WHIM-WT patients described previously.

Inhibitory blockade of CXCR4 signaling using perixafor (or AMD3100) is beneficial in WHIM patients [35]. This recent finding highlights the importance of understanding the CXCL12/CXCR4 signaling pathway for therapeutic purposes in WHIM and in other pathophysiologic conditions involving the marrow, such as HSC mobilization and transplantation [24]. Our data suggest that selective kinase targeting of GRK3 may serve additionally as a potential therapeutic target for these disorders.

AUTHORSHIP

T.K.T. performed the internalization experiments, the arthritis experiments, the chemotaxis experiments, and the flow cytometry experiments of blood and paw, wrote the manuscript, and designed the experiments. M.J.B. designed and performed flow cytometry experiments of BM and provided critical review of the manuscript. R.G.T. and M.W.M. performed the qRT-PCR experiments. D.S.S. performed the phospho-ERK experiments. O.F. performed the histopathology examinations and provided critical review of the manuscript. D.A.E. designed and performed the statistical curve analysis and provided critical review of the manuscript. W.E.L. performed the stem-cell flow cytometry experiments and a critical review of the manuscript. N.J.C. provided contributions toward the stem-cell experimental design and a critical review of the manuscript. D.M.L. and D.P. provided contributions toward the K/BxN experimental design and analysis and a critical review of the manuscript. D.P.S. provided insight into experimental design of the phospho-ERK experiments and construction of the manuscript and added additional writing and critical review of the manuscript.

ACKNOWLEDGMENTS

We acknowledge support from U.S. National Institutes of Health Grants K01AI091863 and K08AI070684, North Carolina Translational and Clinical Sciences (NC TraCS) pilot project via support from U.S. National Institutes of Health Clinical and Translational Science Award UL1TR000083, and R03AR059286. We thank R. J. Lefkowitz (Duke University) for generously providing the GRK3−/− mouse strain.

DISCLOSURES

T.K.T. consults for Hoffmann-La Roche as an independent adjudicator of Phase 1/2/3 clinical-trial patient allergic reactions to study drugs. D.P. and D.M.L. work for Novartis Industries.

REFERENCES

1. Murdoch, C., Finn, A. (2000) Chemokine receptors and their role in inflammation and infectious diseases. *Blood* **95,** 3032–3043.
2. Balabanian, K., Lagane, B., Pablos, J. L., Laurent, L., Planchenault, T., Verola, O., Lebbe, C., Kerob, D., Dupuy, A., Hermine, O., Nicolas, J. F., Latger-Cannard, V., Bensoussan, D., Bordigoni, P., Baleux, F., Le Deist, F., Virelizier, J. L., Arenzana-Seisdedos, F., Bachelerie, F. (2005) WHIM syndromes with different genetic anomalies are accounted for by impaired CXCR4 desensitization to CXCL12. *Blood* **105,** 2449–2457.
3. Hernandez, P. A., Gorlin, R. J., Lukens, J. N., Taniuchi, S., Bohinjec, J., Francois, F., Klotman, M. E., Diaz, G. A. (2003) Mutations in the chemokine receptor gene CXCR4 are associated with WHIM syndrome, a combined immunodeficiency disease. *Nat. Genet.* **34,** 70–74.
4. Balabanian, K., Levoye, A., Klemm, L., Lagane, B., Hermine, O., Harriague, J., Baleux, F., Arenzana-Seisdedos, F., Bachelerie, F. (2008) Leukocyte analysis from WHIM syndrome patients reveals a pivotal role for GRK3 in CXCR4 signaling. *J. Clin. Invest.* **118,** 1074–1084.
5. Lefkowitz, R. J. (1998) G protein-coupled receptors. III. New roles for receptor kinases and β-arrestins in receptor signaling and desensitization. *J. Biol. Chem.* **273,** 18677–18680.
6. Benovic, J. L., Onorato, J. J., Arriza, J. L., Stone, W. C., Lohse, M., Jenkins, N. A., Gilbert, D. J., Copeland, N. G., Caron, M. G., Lefkowitz, R. J. (1991) Cloning, expression, and chromosomal localization of β-adrenergic receptor kinase 2. A new member of the receptor kinase family. *J. Biol. Chem.* **266,** 14939–14946.
7. Haribabu, B., Snyderman, R. (1993) Identification of additional members of human G-protein-coupled receptor kinase multigene family. *Proc. Natl. Acad. Sci. USA* **90,** 9398–9402.
8. Busillo, J. M., Armando, S., Sengupta, R., Meucci, O., Bouvier, M., Benovic, J. L. (2010) Site-specific phosphorylation of CXCR4 is dynamically regulated by multiple kinases and results in differential modulation of CXCR4 signaling. *J. Biol. Chem.* **285,** 7805–7817.
9. Mueller, W., Schutz, D., Nagel, F., Schulz, S., Stumm, R. (2013) Hierarchical organization of multi-site phosphorylation at the CXCR4 C terminus. *PLoS One* **8,** e64975.
10. McCormick, P. J., Segarra, M., Gasperini, P., Gulino, A. V., Tosato, G. (2009) Impaired recruitment of Grk6 and β-arrestin 2 causes delayed internalization and desensitization of a WHIM syndrome-associated CXCR4 mutant receptor. *PLoS One* **4,** e8102.
11. Beaussant Cohen, S., Fenneteau, O., Plouvier, E., Rohrlich, P. S., Daltroff, G., Plantier, I., Dupuy, A., Kerob, D., Beaupain, B., Bordigoni, P., Fouyssac, F., Delezoide, A. L., Devouassoux, G., Nicolas, J. F., Bensaid, P., Bertrand, Y., Balabanian, K., Chantelot, C. B., Bachelerie, F., Donadieu, J. (2012) Description and outcome of a cohort of 8 patients with WHIM syndrome from the French Severe Chronic Neutropenia Registry. *Orphanet. J. Rare Dis.* **7,** 71.
12. Gorlin, R. J., Gelb, B., Diaz, G. A., Lofsness, K. G., Pittelkow, M. R., Fenyk J. R., Jr., (2000) WHIM syndrome, an autosomal dominant disorder: clinical, hematological, and molecular studies. *Am. J. Med. Genet.* **91,** 368–376.
13. Walker, J. K., Peppel, K., Lefkowitz, R. J., Caron, M. G., Fisher, J. T. (1999) Altered airway and cardiac responses in mice lacking G protein-coupled receptor kinase 3. *Am. J. Physiol.* **276,** R1214–R1221.
14. Peppel, K., Boekhoff, I., McDonald, P., Breer, H., Caron, M. G., Lefkowitz, R. J. (1997) G protein-coupled receptor kinase 3 (GRK3) gene disruption leads to loss of odorant receptor desensitization. *J. Biol. Chem.* **272,** 25425–25428.
15. Xu, M., Petraschka, M., McLaughlin, J. P., Westenbroek, R. E., Caron, M. G., Lefkowitz, R. J., Czyzyk, T. A., Pintar, J. E., Terman, G. W., Chavkin, C. (2004) Neuropathic pain activates the endogenous κ opioid system in mouse spinal cord and induces opioid receptor tolerance. *J. Neurosci.* **24,** 4576–4584.
16. Graziewicz, M. A., Tarrant, T. K., Buckley, B., Roberts, J., Fulton, L., Hansen, H., Orum, H., Kole, R., Sazani, P. (2008) An endogenous TNF-α antagonist induced by splice-switching oligonucleotides reduces inflammation in hepatitis and arthritis mouse models. *Mol. Ther.* **16,** 1316–1322.
17. Travlos, G. S. (2006) Histopathology of bone marrow. *Toxicol. Pathol.* **34,** 566–598.
18. Ueda, Y., Kondo, M., Kelsoe, G. (2005) Inflammation and the reciprocal production of granulocytes and lymphocytes in bone marrow. *J. Exp. Med.* **201,** 1771–1780.
19. Perruche, S., Kleinclauss, F., Lienard, A., Robinet, E., Tiberghien, P., Saas, P. (2004) A single-platform approach using flow cytometry and

microbeads to evaluate immune reconstitution in mice after bone marrow transplantation. *J. Immunol. Methods* **294,** 53–66.
20. Tarrant, T. K., Liu, P., Rampersad, R. R., Esserman, D., Rothlein, L. R., Timoshchenko, R. G., McGinnis, M. W., Fitzhugh, D. J., Patel, D. D., Fong, A. M. (2012) Decreased Th17 and antigen-specific humoral responses in CX(3) CR1-deficient mice in the collagen-induced arthritis model. *Arthritis Rheum.* **64,** 1379–1387.
21. Whitlock, C. A., Witte, O. N. (1981) Abelson virus-infected cells can exhibit restricted in vitro growth and low oncogenic potential. *J. Virol.* **40,** 577–584.
22. Balabanian, K., Brotin, E., Biajoux, V., Bouchet-Delbos, L., Lainey, E., Fenneteau, O., Bonnet, D., Fiette, L., Emilie, D., Bachelerie, F. (2012) Proper desensitization of CXCR4 is required for lymphocyte development and peripheral compartmentalization in mice. *Blood* **119,** 5722–5730.
23. Broxmeyer, H. E., Orschell, C. M., Clapp, D. W., Hangoc, G., Cooper, S., Plett, P. A., Liles, W. C., Li, X., Graham-Evans, B., Campbell, T. B., Calandra, G., Bridger, G., Dale, D. C., Srour, E. F. (2005) Rapid mobilization of murine and human hematopoietic stem and progenitor cells with AMD3100, a CXCR4 antagonist. *J. Exp. Med.* **201,** 1307–1318.
24. Kang, Y., Chen, B. J., Deoliveira, D., Mito, J., Chao, N. J. (2010) Selective enhancement of donor hematopoietic cell engraftment by the CXCR4 antagonist AMD3100 in a mouse transplantation model. *PLoS One* **5,** e11316.
25. Lagane, B., Chow, K. Y., Balabanian, K., Levoye, A., Harriague, J., Planchenault, T., Baleux, F., Gunera-Saad, N., Arenzana-Seisdedos, F., Bachelerie, F. (2008) CXCR4 dimerization and β-arrestin-mediated signaling account for the enhanced chemotaxis to CXCL12 in WHIM syndrome. *Blood* **112,** 34–44.
26. Korganow, A. S., Ji, H., Mangialaio, S., Duchatelle, V., Pelanda, R., Martin, T., Degott, C., Kikutani, H., Rajewsky, K., Pasquali, J. L., Benoist, C., Mathis, D. (1999) From systemic T cell self-reactivity to organ-specific autoimmune disease via immunoglobulins. *Immunity* **10,** 451–461.
27. Wipke, B. T., Allen, P. M. (2001) Essential role of neutrophils in the initiation and progression of a murine model of rheumatoid arthritis. *J. Immunol.* **167,** 1601–1608.
28. Tarrant, T. K., Rampersad, R. R., Esserman, D., Rothlein, L. R., Liu, P., Premont, R. T., Lefkowitz, R. J., Lee, D. M., Patel, D. D. (2008) Granulocyte chemotaxis and disease expression are differentially regulated by GRK subtype in an acute inflammatory arthritis model (K/BxN). *Clin. Immunol.* **129,** 115–122.
29. Rampersad, R. R., Tarrant, T. K., Vallanat, C. T., Quintero-Matthews, T., Weeks, M. F., Esserman, D. A., Clark, J., Di Padova, F., Patel, D. D., Fong, A. M., Liu, P. (2011) Enhanced Th17-cell responses render CCR2-deficient mice more susceptible for autoimmune arthritis. *PLoS One* **6,** e25833.
30. Van Vollenhoven, R. F., Fleischmann, R., Cohen, S., Lee, E. B., Garcia Meijide, J. A., Wagner, S., Forejtova, S., Zwillich, S. H., Gruben, D., Koncz, T., Wallenstein, G. V., Krishnaswami, S., Bradley, J. D., Wilkinson, B. ORAL Standard Investigators (2012) Tofacitinib or adalimumab versus placebo in rheumatoid arthritis. *N. Engl. J. Med.* **367,** 508–519.
31. Fong, A. M., Premont, R. T., Richardson, R. M., Yu, Y. R., Lefkowitz, R. J., Patel, D. D. (2002) Defective lymphocyte chemotaxis in β-arrestin2- and GRK6-deficient mice. *Proc. Natl. Acad. Sci. USA* **99,** 7478–7483.
32. Vroon, A., Heijnen, C. J., Raatgever, R., Touw, I. P., Ploemacher, R. E., Premont, R. T., Kavelaars, A. (2004) GRK6 deficiency is associated with enhanced CXCR4-mediated neutrophil chemotaxis in vitro and impaired responsiveness to G-CSF in vivo. *J. Leukoc. Biol.* **75,** 698–704.
33. Ma, Q., Jones, D., Borghesani, P. R., Segal, R. A., Nagasawa, T., Kishimoto, T., Bronson, R. T., Springer, T. A. (1998) Impaired B-lymphopoiesis, myelopoiesis, and derailed cerebellar neuron migration in CXCR4- and SDF-1-deficient mice. *Proc. Natl. Acad. Sci. USA* **95,** 9448–9453.
34. Latger-Cannard, V., Bensoussan, D., Bordigoni, P. (2006) The WHIM syndrome shows a peculiar dysgranulopoiesis: myelokathexis. *Br. J. Haematol.* **132,** 669.
35. McDermott, D. H., Liu, Q., Ulrick, J., Kwatemaa, N. , Anaya-O'Brien, S., Penzak, S. R., Filho, J. O., Priel, D. A., Kelly, C., Garofalo, M., little, P., Marquesen, M. M., Hilligoss, D., Decastro, R., Fleisher, T. A., Kuhns, D. B., Malech, H. L., Murphy, P. M. (2011) The CXCR4 antagonist plerixafor corrects panleukopenia in patients with WHIM syndrome. *Blood* **118,** 4957–4962.

KEY WORDS:
chemokine receptor · hematopoiesis · granulocytes · arthritis